

Interference Effects of Via Interconnect in Three Layer Printed Circuit Board

Avali Ghosh, Sisir Kumar Das, and Annapurna Das

Guru Nanak Institute of Technology
JIS Group, 157/F, Nilgunj Road, Sodepur, Kolkata-700114, India
avalighosh@gmail.com, dean_gnit@jisgroup.org, director_gnit@jisgroup.org

Abstract — Cylindrical vias are commonly used for interconnection in multilayered Printed Circuit Board (PCB) design. The RF current through vias causes radiated interference to adjacent traces. This paper describes an analytical method of computing the radiation from cylindrical via using the electromagnetic theory. Three layer printed circuit board consisting of three traces on the top of a dielectric substrate, a middle orthogonal trace and a ground plane at the bottom, is considered. The RF voltage coupling at the terminations of the traces due to the near field radiation from the via is computed. The reactive couplings between the traces are determined from the parasitic elements using transmission line equations. The total coupling obtained from analytical method is compared with those of modeling and simulation with Ansoft HFSS software tool. The total crosstalk is also measured using an available Network Analyzer. A good agreement is found. The changes of radiated coupling with the change of position of via, trace separation and trace length are also investigated. This paper shows that the analytical method is a useful tool for predicting interference in PCB without using expensive simulation software.

Index Terms — Crosstalk, electromagnetic compatibility, PCB, transmission line, via, via inductance.

I. INTRODUCTION

Analysis of reactive cross-talk between the traces in multilayer printed circuit board is described by Paul [1] using transmission line theory and results are well documented. In multilayer PCB, vias are placed to interconnect signals from one layer to another. Their locations are optimized for desired circuit operation with signal integrity and Electromagnetic Compatibility (EMC). Very costly software tools are utilized for this purpose. The effects of via interconnects are analyzed by many authors [2-12]. Pucel [2] developed an empirical formula for via inductance using image concept. Goldfarb and Pucel [3] developed empirical formula for via inductance based on measurements and numerical simulation. Cui et al. [4] described EMI problem due to via transitions through the DC power bus. Li et al.

[5] and Suntives et al. [6] have shown shielding of interference between PCB traces using an array of vias in a trace. Nam et al. [7] shown EMI mitigation in PCB using shorting vias around the signal via. Ndip et al. [8] described techniques to solve electromagnetic reliability problem due to return current paths through via by introducing layer stack up scheme. Jiang and Fan [9] has given an intrinsic via circuit model through rigorous electromagnetic analysis. Wu and Fan [10] analytically predicted crosstalk among multiple vias between infinitely large parallel planes. Pan and Fan [11] given an equivalent multi-conductor transmission line model to characterize via structures in multi-layer PCBs for signal integrity in high speed digital circuits. Isidoro-Munoz et al. [12] presented closed-form expressions for the via-pad capacitance and via-traces inductance for the performance assessment and optimization of signal integrity. None of the above publications described the analysis of radiation from via and its effects on the adjacent lines. Some results of radiation coupling from via placed in a fixed position are presented by the authors in international conferences [14,15].

In this paper the effects of via (interconnect) in a three layer PCB are described along with the reactive crosstalk between the traces. The three layer board consists of three parallel traces (Trace1, 2 and 3) on the top of a FR4 dielectric substrate (copper clad FR4 glass epoxy, S3110, CEM-1), a second layer trace (Trace 4) which is orthogonal to the top traces, and a bottom layer of ground plane as shown in Fig. 1. The single layer thickness of the substrate is h and having dielectric constant ϵ_r . The trace 1 and trace 4 are interconnected through a thin cylindrical via of diameter d . The RF current through via radiates electromagnetic signal in the hybrid medium formed by the solid dielectric substrate and the air on the top. The radiated magnetic field produces induced RF current on the adjacent traces. The net current gives rise to interference voltage at the ports terminated with matched loads.

Since the via model considered here does not have pad, and the length is very small due to thin substrate, the equivalent circuit of the via is an inductance. This

unknown inductance is computed from the transmission line model of the traces and using Ansoft HFSS software tool. For excitation of trace 1, the RF current through via is found and the radiation from the via is determined using Helmholtz equation in spherical domain [16]. The total interference coupling at the ports of the adjacent traces is the sum of radiated coupling voltage and the reactive coupling voltage. The reactive coupling is computed using empirical formulae of parasitic inductance and capacitance given by Sakurai [13].

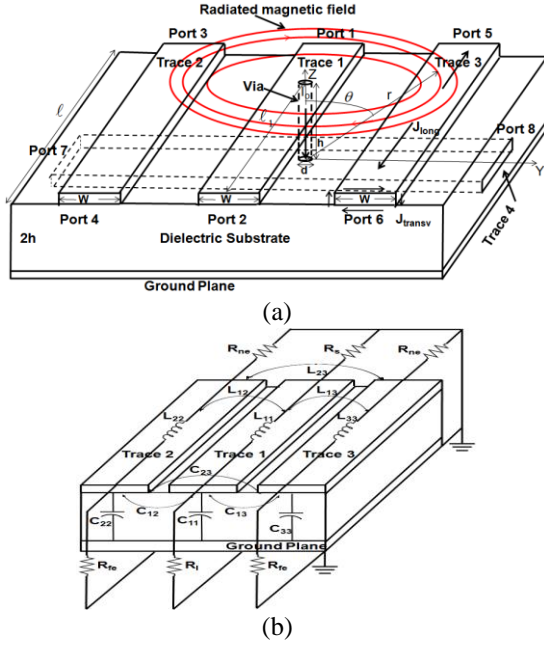


Fig. 1. Multilayer PCB structure: (a) via radiation coupling, and (b) reactive cross-talk coupling (via and orthogonal trace 4 are not shown).

The analytical values of the near field radiated coupling, reactive coupling and the total coupling are computed using MATLAB. Ansoft HFSS modeling and simulation of the structure is also done to find the resultant interference coupling on the traces at different frequencies for different locations of the via, trace length and trace spacing. Modeling and simulation results are compared with those obtained from analytical method and found good agreement. Experimental verification is also conducted for via position at the center of the trace along the length and results are found agreed well with those of simulation and analytical methods.

II. METHODS OF ANALYSIS

A. Analysis of radiation coupling from via RF current

As shown in Fig. 1, trace 1 is excited by RF current at Port 1. All the traces have width W and are matched

terminated by their characteristic impedances (50 ohm). A z -directed small via is a small dipole inside the substrate which radiates spherical waves in the hybrid medium around the via having non-zero field components E_r , E_θ and H_ϕ correspond to TM_r modes. Scalar magnetic potential A_r corresponding to these field components satisfies Helmholtz equations outside the via [16]:

$$\nabla^2 A_r + k^2 A_r = 0. \quad (1)$$

Here $k = k_0 \sqrt{\epsilon_e}$ in the hybrid medium consisting of dielectric substrate and air above it,

$$A_r = \frac{jkI_0h}{4\pi} \hat{H}_1^{(2)}(kr) P_1(\cos\theta), \quad (2)$$

and ϵ_e is the effective dielectric constant of the hybrid medium given by [17]:

$$\epsilon_e = \frac{\epsilon_r + 1}{2} + \frac{\epsilon_r - 1}{2} \left(1 + \frac{12h}{W}\right)^{-1/2}. \quad (3)$$

In (2) $\hat{H}_1^{(2)}(kr)$ is spherical Hankle function of 2nd kind, $P_1(\cos\theta)$ is Legendre polynomial of degree 1, and I_0 is RF current through via which will be determined from the via equivalent circuit and transmission line model of the traces.

Since the via is orthogonal to the traces on the top layer and on the middle layer, to a first degree of approximation, the scattering effects of these traces for the radiation from via is neglected. The magnetic field component H_ϕ induces transverse and longitudinal components of RF current on the surfaces of these traces. From (1) and (2), the radiated magnetic near field component:

$$H_\phi = -\frac{1}{r} \frac{\partial A_r}{\partial \theta} = \frac{jkI_0h}{4\pi r} \hat{H}_1^{(2)}(kr) \sin\theta. \quad (4)$$

Since the ground plane is considered as perfectly conducting, its effect on this emitted field is taken by replacing the ground plane with the image of the via (Fig. 2 (a)). The resultant radiated field component can be obtained from (4) for contributions of via and its image.

$$H_\phi = \frac{jkI_0h}{4\pi} \left[\frac{1}{r_1} \hat{H}_1^{(2)}(kr_1) \sin\theta_1 + \frac{1}{r_2} \hat{H}_1^{(2)}(kr_2) \sin\theta_2 \right]. \quad (5)$$

We can write [16]:

$$\hat{H}_n^{(2)}(kr) = \sqrt{\frac{\pi kr}{2}} H_{n+1/2}^{(2)}(kr), \quad (5a)$$

where $H_{n+1/2}^{(2)}(kr)$ is the cylindrical Hankle function.

From the geometry (Fig. 2 (a)), for field point $P(x, y, z)$,

$$r_1 = \sqrt{y^2 + (x - \ell_1)^2}, \quad (5b)$$

$$r_2 = \sqrt{r_1^2 + (3h)^2}, \quad (5c)$$

$$\theta_1 = \tan^{-1}\left(\frac{\ell_1}{2h}\right) \text{ and } \theta_2 = \pi - \theta_1, \quad (5d)$$

$$\cos\phi = \frac{-x}{r} = \frac{-x}{\sqrt{x^2 + y^2}}, \quad (5e)$$

$$\text{and } \cos\theta = \frac{(3/2)h}{r}. \quad (5f)$$

The induced surface current density on the top surface of the trace 2:

$$\vec{J}_{top} = \hat{z} x \hat{\phi} H_{\phi t} = -H_{\phi t} (\hat{x} \cos\phi + \hat{y} \sin\phi). \quad (6)$$

On the bottom surface of trace 2:

$$\vec{J}_{bottom} = -\hat{z} x \hat{\phi} H_{\phi b} = H_{\phi b} (\hat{x} \cos\phi + \hat{y} \sin\phi), \quad (7)$$

where suffices ϕt and ϕb represent top and bottom surfaces, respectively.

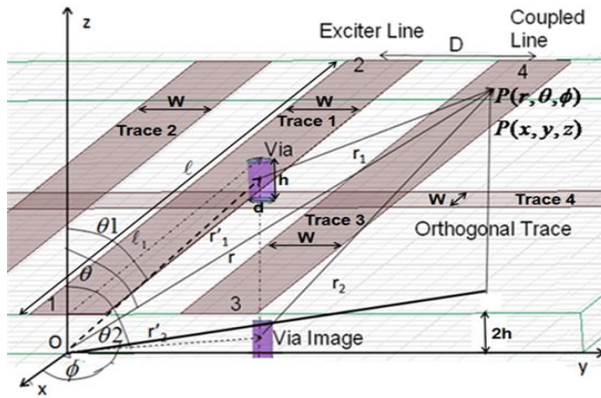


Fig. 2. Isometric view of the analytical model with via and its image below ground plane ($W=6.2\text{mm}$, $\ell_1=200\text{mm}$, $\ell_1=100\text{mm}$, $h=1.6\text{mm}$, $d=1\text{mm}$).

On the side outermost surface of trace 2:

$$\vec{J}_{rs} = \hat{y} x (\hat{\phi} H_{\phi}) = \hat{z} \sin\phi H_{\phi}. \quad (8)$$

On the side innermost surface of trace 2:

$$\vec{J}_{ls} = -\hat{y} x (\hat{\phi} H_{\phi}) = -\hat{z} \sin\phi H_{\phi}. \quad (9)$$

Therefore, it is seen that there is circulatory transverse current and also longitudinal current induced on the adjacent traces due to RF current through via along z . In PCB, the trace thickness is extremely small compare to width/wavelength. Therefore, in this analysis we can neglect the current on the side surfaces of the traces. The net current on top and bottom surfaces of the traces results in radiated coupling of signal at Ports 3, 4, 5 and 6 which can be obtained from (6) and (7). The resultant component of current density at P on a trace is given by:

$$J = \left| \vec{J}_{bottom} + \vec{J}_{top} \right| = H_{\phi b} - H_{\phi t}. \quad (10)$$

Therefore, the net current flow per unit length through adjacent victim trace can be expressed as:

$$I = \int_{D-W/2}^{D+W/2} (H_{\phi b} - H_{\phi t}) dy. \quad (11a)$$

The coupled voltages at ports are obtained by multiplying this current with port impedances $Z_L = Z_0$:

$$V = Z_L \times I. \quad (11b)$$

Equations (11a) and (11b) can be solved after determining the unknown excitation current I_0 through via.

B. Transmission line model of trace with equivalent circuit of via to find I_0

In general, the design of PCB is made using pad on a trace for connection of via with the associated trace. In this analytical model an assumption is made that the via with non-zero diameter $d \ll \lambda$ is connected between Trace 1 and 4 without pad. Therefore, the via offers an inductive path ($j\omega L_v$) as explained in Fig. 3 using transmission line model of the traces along with equivalent circuit of via, where L_v is the inductance of via.

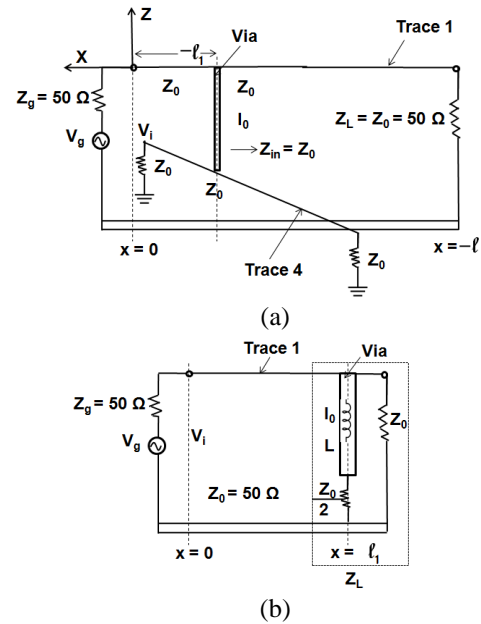


Fig. 3. (a) Equivalent circuit of via between traces 1 and 4, and (b) transformed equivalent circuit.

Considering a uniform lossless transmission line (Trace 1) of characteristic impedance $Z_0\Omega$ and length ℓ mm, excited at $x=0$ with a matched voltage source V_g , the equivalent load at the via point $x = -\ell_1$ is (Fig. 3),

$$Z_L = \frac{(j\omega L_v + Z_0/2)Z_0}{(j\omega L_v + Z_0/2) + Z_0}. \quad (12)$$

Based on formula developed by Pucel [2], the via inductance is given by:

$$L_v = \frac{\mu_0}{4\pi} \left[2h \cdot \ln \left(\frac{2h + \sqrt{\frac{d^2}{4} + (2h)^2}}{d/2} \right) + \left(\frac{d}{2} - \sqrt{\frac{d^2}{4} + (2h)^2} \right) \right]. \quad (13)$$

The line voltage at via point can be expressed by:

$$V(-\ell_1) = V_i (e^{+j\beta\ell_1} + \Gamma e^{-j\beta\ell_1}). \quad (14)$$

Here V_i = input signal voltage,

$$\beta = \frac{2\pi}{\lambda_e}, \quad \lambda_e = \frac{\lambda_0}{\sqrt{\epsilon_e}}, \quad \Gamma = \frac{Z_L - Z_0}{Z_L + Z_0}. \quad (15)$$

For excitation at Port 1, the via current can be calculated using (12) to (15) as:

$$I_0 = \frac{V(-\ell_1)}{j\omega L_v + Z_0/2}. \quad (16)$$

This I_0 is used in Equation 4 to find the radiated magnetic field and subsequently radiated coupling voltage at the trace end from (11a) and (11b).

C. Reactive and total coupling to the adjacent trace

There are direct crosstalk from the source trace to the adjacent parallel lines resulting in near end and far end cross-talk voltages due to reactive coupling. Since middle layer trace is orthogonal to top layer traces, there is no direct coupling to middle layer. The electrical equivalent circuit for inductive and capacitive coupling is shown in Fig. 1 (b).

At low frequency side of GHz range, crosstalk due to reactive coupling is well described by Paul [1] for lossless lines and are expressed by:

$$V_{ne} = \frac{j\omega R_{ne}}{(R_{ne} + R_{fe})(R_s + R_\ell)} [L_{12} + R_{fe} R_\ell C_{12}], \quad (17)$$

$$V_{fe} = \frac{j\omega R_{fe}}{(R_{ne} + R_{fe})(R_s + R_\ell)} [-L_{12} + R_{ne} R_\ell C_{12}], \quad (18)$$

where V_{ne} and V_{fe} are the reactive coupling due to via at Ports 3 and 4, respectively, $R_{ne} = R_{fe} = 50\Omega$, C_{12} and L_{12} are total mutual capacitance and inductance, respectively, per unit length. The capacitances and inductances are computed from the expressions given

by Sakurai [13]. The capacitance matrix can be written as:

$$[C] = \begin{bmatrix} (C_{11} + 2C_{12}) & -C_{12} & -C_{12} \\ -C_{12} & (C_{11} + C_{12}) & -C_{23} \\ -C_{12} & -C_{23} & (C_{11} + C_{12} + C_{23}) \end{bmatrix}, \quad (19)$$

where C_{ij} is the capacitance between the trace i and trace j , and C_{ii} is the capacitance between the trace i and the ground. Here $C_{23} = 0$ and $C_{12} = C_{13}$ for symmetry.

Since the inductance is not influenced by the lossless dielectric substrate the line inductance is derived from $[C]$ using the following relation:

$$[L] = \mu_0 \epsilon_0 [C]^{-1}. \quad (20)$$

The total coupled voltage at the port is the sum of the direct crosstalk voltage and the voltage due to radiation coupling from the via:

$$V_{31} = V_{r3} + V_{ne} \text{ and } V_{41} = V_{r4} + V_{fe}, \quad (21)$$

where, V_{r3} and V_{r4} are the radiated coupling due to via at Ports 3 and 4 respectively.

D. Simulation and Modeling

The PCB of Fig. 1 is simulated using Ansoft HFSS software with FR4 substrate having $\epsilon_r = 4.4$, $\tan \delta = 0.02$ and single layer thickness $h = 1.6\text{mm}$. All the traces have length 200mm, and are designed for 50 ohm impedance. The lines are matched terminated. A cylindrical via having diameter of 1mm, located at an arbitrary distance ℓ_1 from the input port, is used to connect the top source trace 1 and middle orthogonal trace 4. Ground plane is at the bottom of the substrate. The simulation and modeling in HFSS tool gives the true coupling, i.e., total coupling due to reactive cross talk and radiation coupling from RF current through via.

III. RESULTS

Following paragraphs describe the results obtained from the analytical, simulation and modeling using HFSS tool and experimental methods. Separate results are shown for radiation coupling, reactive coupling and total coupling (combined coupling due to radiation and reactive coupling).

A. Radiation coupling from via RF current

The radiated coupled voltage vs frequency at a Port 4 for 50 ohm termination is obtained from (11) and (16) using MATLAB, and the result is shown in Fig. 4, when via is placed at the middle along the length of the trace. The radiated couplings at all other ports can similarly be obtained.

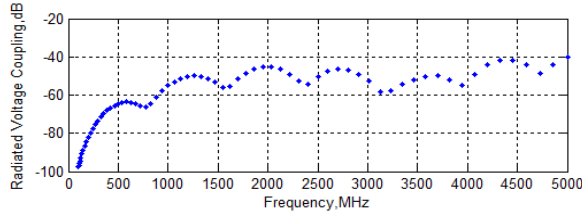


Fig. 4. Radiated coupled voltage vs. frequency using analytical method ($\ell = 200\text{mm}$, $\ell_1 = 100\text{mm}$).

B. Reactive and total coupling to the adjacent trace

The reactively coupled cross-talk voltages V_{ne} and V_{fe} are computed from (17) to (20), using MATLAB and the results are shown in Fig 5. It is seen that both the couplings increase with frequency.

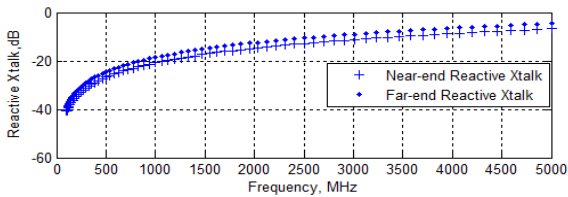


Fig. 5. Reactively coupled crosstalk voltages vs. frequency using analytical method ($\ell = 200\text{mm}$, $\ell_1 = 100\text{mm}$).

Finally, the total coupled voltage vs. frequency, expressed by (21), is shown in Fig. 6. It is seen from Fig. 4, Fig. 5 and Fig. 6, that the reactive coupling predominates coupling due to via radiation.

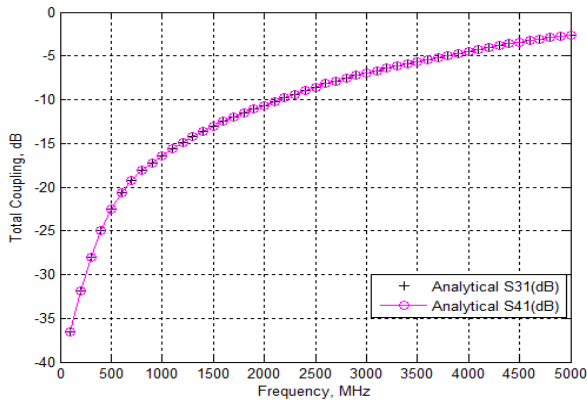


Fig. 6. Total coupled voltage vs. frequency using analytical method ($\ell = 200\text{mm}$, $\ell_1 = 100\text{mm}$).

C. Experimental and simulation results of coupling

The coupling parameters S31 (near-end) and S41 (far-end) are measured by using Rohde & Schwarz

ZVH4 Analyzer with the via at the center of the source trace as shown in Fig. 7.

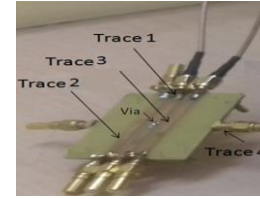


Fig. 7. PCB with via is at centre of Trace 1.

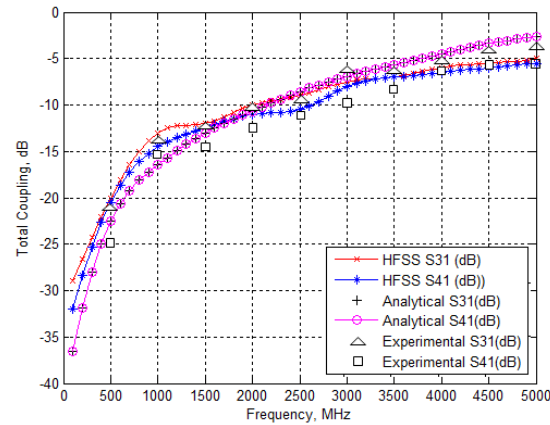


Fig. 8. Total coupled voltage vs. frequency (HFSS, analytical and experimental) when via is at centre of Trace 1.

The HFSS, analytical and experimental results of total coupled voltage at near end and far end ports of the adjacent victim trace versus frequency are compared and shown in Fig. 8. It is found that there is some deviation of 2-3 dB between the results which may be due to some assumptions made in the analytical method. At lower part of the frequencies, the deviation is slightly more. This may be due to the line losses which cannot be neglected at lower frequencies because propagation constant becomes complex and due to some experimental error.

D. Results of change in coupling with via position and line dimensions

The changes of radiated coupling with the other parameters, such as, (i) change of position of via, (ii) trace separation and (iii) trace length are investigated by using analytical method as discussed above. The effect of change of position of via on radiated coupling is shown in Fig. 9. It is observed that when the via is at the center along the length, then the radiated coupling voltage due to via is minimum and when it approaches towards the end of the traces, it increases.

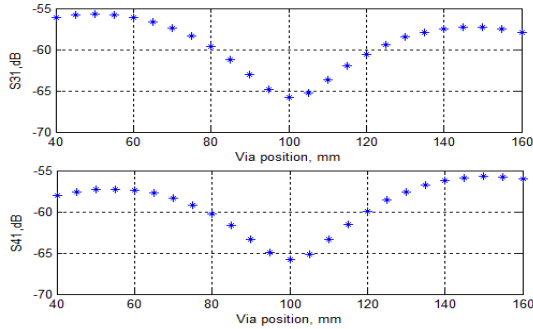


Fig. 9. Radiated coupling voltage vs. via position using analytical method.

The effect of trace length on radiated coupling is shown in Fig. 10. It is seen that when the length is increased the radiated coupling voltage is decreased.

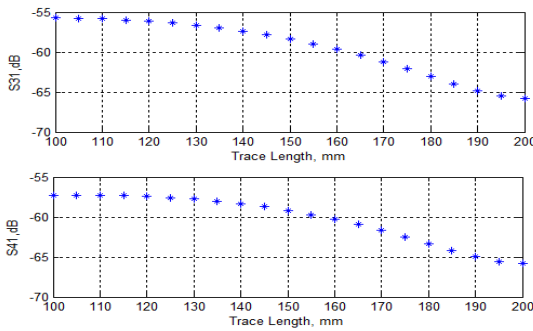


Fig. 10. Radiated coupling voltage vs. trace length using analytical method.

Figure 11 shows that when the trace separation is increased, the analytical results of radiated coupling voltage at different ports of the adjacent trace decrease with separation as expected.

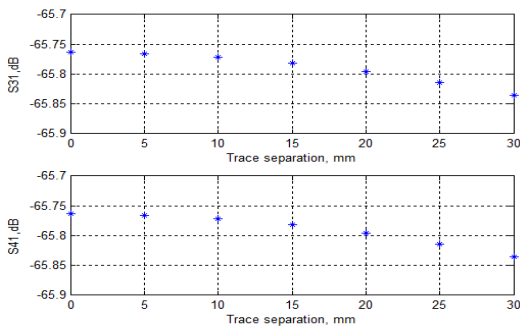


Fig. 11. Radiated coupling voltage vs. trace separation using analytical method.

The HFSS simulations are also carried out for (a) different positions of the via along the trace, (b) different trace lengths, and (c) different separation distances

between the traces. The simulated and analytical results of total coupling voltages at different ports of the traces for these cases are shown in Fig. 12 for two frequencies, 350 and 600 MHz. It is seen that the analytical results agree well with those of HFSS simulation and modeling with a maximum deviation of 15%.

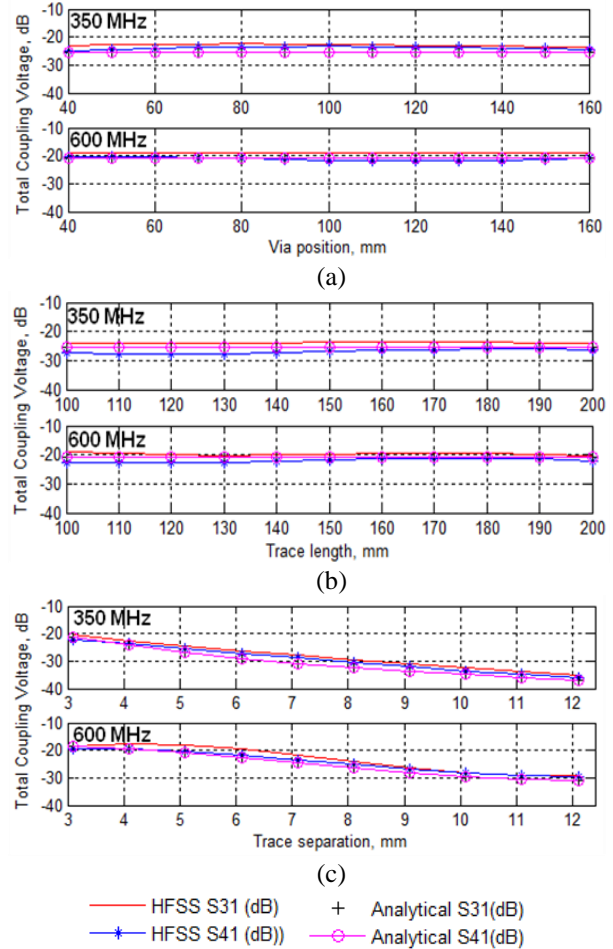


Fig. 12. Variation of coupling voltage: (a) with via position, (b) with trace length, and (c) with trace separation.

IV. DISCUSSION AND CONCLUSION

This paper describes radiation effect of via interconnect and reactive crosstalk between adjacent traces in a three layer PCB. The three layer PCB consists of three traces on the top, a middle orthogonal trace and a ground plane at the bottom. Centre trace 1 on the top layer is the source and interconnected to the orthogonal trace 4 through the via. The dielectric substrate used in the PCB is FR4-epoxy ($\epsilon_r = 4.4$). Each layer has thickness of 1.6mm. The traces are designed for 50 ohm impedance and terminated with matched loads. Analysis of radiation due to RF current through via is carried out using Helmholtz equation in spherical domain in hybrid

medium consisting of dielectric substrate and air on the top. The coupling of near field radiation from the via to the traces are calculated in terms of voltages due to the induced current on the traces. The total coupled voltage at a port is the sum of the radiated coupled voltage due to via radiation and the reactive crosstalk voltage from the adjacent traces due to line parasitic. It is seen that the reactive coupling is predominant over the radiated coupling voltage due to via.

Paper also describes the Ansoft HFSS analysis of the structure which takes care of both cross-talk due to reactive coupling between adjacent traces and radiated coupling due to via current. HFSS uses the Finite Element Method (FEM) in which automated adaptive meshing is generated. At the point of discontinuities smaller size of meshes and in the region of less complicated geometries, bigger meshes are generated. This helps to converge to the desired accuracy of the solution faster.

In general, total crosstalk increases with frequency. The via has little effect on the reactive coupling due to its small size and low values of inductance L_v . However, the effects of the variation in the position of via, change of trace length and trace separation, on the radiated coupling are also analytically investigated and verified with the help of HFSS simulation in this paper. It is seen that the position of the via alters the radiated coupling value giving a minimum when the via is at the center position of the trace length. It is observed that as the length and trace separation is increased, the radiation coupling from via is decreased.

The total crosstalk is measured using a network analyzer when the via is at the center of the length of the source trace 1. The overall observation shows that the results obtained with analytical and experimental methods have good agreement with a maximum deviation of 2-3 dB from those of HFSS simulation. The deviation of results may be due to some error in experimentation and assumptions made in the theory. The authenticity of the analytical work is verified by using very accurate modeling and simulation software tool Ansoft HFSS. However, deviation is maximum (> 5 dB) at lower parts of the frequency. This may be due to the line losses which are ignored in the theory. The analytical method described here shows that without using expensive software tools, interference coupling can be estimated applying electromagnetic theory.

REFERENCES

- [1] C. R. Paul, *Introduction to Electromagnetic Compatibility*. John Wiley & Sons, Inc., 1992.
- [2] R. Pucel, *Gallium Arsenide Technology*. D. Ferry, Ed., Indianapolis, IN: Howard W. Sams and Co., Ch. 6, pp. 216, 1985.
- [3] M. E. Goldfarb and R. A. Pucel, "Modeling via hole grounds in microstrip," *IEEE Microwave Guided Wave Letter*, vol. 1, no. 6, pp. 135-137, June 1991.
- [4] W. Cui, X. Ye, B. Archambeault, D. White, M. Li, and J. L. Drewniak, "EMI resulting from signal via transitions through the DC power bus," *2000 IEEE International Symposium on Electromagnetic Compatibility*, vol. 2, pp. 821-826, Aug. 21-25, 2000.
- [5] S. Li, Y. Liu, Z. Song, and H. Hu, "Analysis of crosstalk of coupled transmission lines by inserting additional traces grounded with vias on printed circuit boards," *Asia Pacific Conference on Environmental Electromagnetics, CEEM'2003*, Hangzhou, China, Nov. 4-7, 2003.
- [6] A. Suntives, A. Khajoeizadeh, and R. Abhari, "Using Via Fences for Crosstalk Reduction in PCB Circuits, 1-4244-0293-X/06/\$20.00(c) 2006 IEEE.
- [7] S. Nam, Y. Kim, J. H. Hur, S. Song, B. J. Lee, and J. Jeong, "Performance analysis of signal vias using virtual islands with shorting vias in multilayer PCBs," *IEEE Transactions on Microwave Theory and Techniques*, vol. 54, no. 4, Part 11315-1324, June 2006.
- [8] I. Ndip, F. Ohnimus, S. Guttowski, and H. Reichl, "Modeling and analysis of return-current paths for microstrip-to-microstrip via transitions," *IEEE Electronic System-Integration Technology Conference (ESTC 2008)*, London, UK, Sep. 1-4, 2008.
- [9] Y.-J. Zhang and J. Fan, "An intrinsic circuit model for multiple vias in an irregular plate pair through rigorous electromagnetic analysis," *IEEE Trans. Microwave Theory Tech.*, vol. 58, no. 8, pp. 2251-2265, Aug. 2010.
- [10] S. Wu and J. Fan, "Analytical prediction of crosstalk among vias in multilayer printed circuit boards," *IEEE Transactions on Electromagnetic Compatibility*, vol. 54, no. 2, Apr. 2012.
- [11] S. Pan and J. Fan, "Characterization of via structures in multilayer printed circuit boards with an equivalent transmission-line model," *IEEE Transactions on Electromagnetic Compatibility*, vol. 54, no. 5, Oct. 2012.
- [12] A. Isidoro-Munoz, R. Torres-Torres, M. A. Tlaxcalteco-Matus, and G. Hernandez-Sosa, "Scalable models to represent the via-pad capacitance and via-traces inductance in multilayer PCB high speed interconnects," *2017 International Conference on Devices, Circuits and Systems (ICDCS)*, 2017.
- [13] T. Sakurai and K. Tamaru, "Simple formulas for two- and three-dimensional capacitances," *IEEE Transactions on Electron Devices*, vol. ED-30, no. 2, Feb. 1983.
- [14] A. Ghosh, S. K. Das, and A. Das, "Analysis of radiation coupling from via in multilayer printed

circuit board traces,” *14th International Conference on Electromagnetic Interference & Compatibility (INCEMIC 2016) and Workshop*, Bengaluru, India, Dec. 8-9, 2016. Electronic ISBN: 978-1-5090-5840-2. DOI: 10.1109/INCEMIC.2016.7921461

- [15] A. Ghosh, S. K. Das, and A. Das, “Analysis of crosstalk in high frequency printed circuit boards in presence of via,” *International Conference on Electromagnetics in Advanced Applications IEEE-APS Topical Conference on Antennas and Propagation in Wireless Communications 2017*, Verona, Italy, Sep. 11-15, 2017. Electronic ISBN: 978-1-5090-4451-1. DOI: 10.1109/ICEAA.2017.8065265
- [16] R. F. Harrington, *Time - Harmonic Electromagnetic Fields*. Donald G. Dudley, Series Editor, Wiley Publication.
- [17] C. A. Balanis, *Advanced Engineering Electromagnetics*. John Wiley & Sons, New York, 1989.



Avali Ghosh, obtained B.E degree from Nagpur University, M.Tech degree from West Bengal University of Technology (MAKAUT) and pursuing Ph.D degree in MAKAUT. Currently she is Assistant Professor in the Department of ECE, GNIT, Kolkata. She is Member of IEEE,

Life Member of ISTE and Society of EMC Engineers (India). Her current interests are microwaves and EMI/EMC.



Sisir Kumar Das, obtained B.Tech, M.Tech and Ph.D degrees from Calcutta University, IIT Kharagpur and Anna University, respectively, in India. He was Faculty in Delhi University during 1977-1980. Das led EMC evaluation and design of electronics products for 28 years under the ministry of communication and IT, Govt. of India, during 1980-2007. Presently he is Prof. and Dean – Research & Administration, GNIT, Kolkata. Das served as Associate Editor for IEEE EMC journal, USA (1994-2000) and now Chief Editor of EMC Journal of Society of EMC Engineers (India). He is Senior Member of IEEE.



Annapurna Das, obtained M.Sc. degree in Physics from University of Calcutta, M.Tech degree in Microwave Electronics and Ph.D degree in Electrical Engineering from the University of Delhi. She worked in the Department of ECE, Anna University during 1985-2007 as Professor. Presently she is Director of GNIT, Kolkata. She is the Life Member of Society of EMC Engineers (India) and ISTE, and Member of IEEE.